

Electronic Supplementary Information

A Fluorescent pH Chemosensor in Strong Acidic Region Based on Intramolecular Charge Transfer (ICT) Effect

Yiqun Tan, Jiancan Yu, Junkuo Gao, Yuanjing Cui, Zhiyu Wang, Yu Yang,* Guodong Qian*

*State Key Laboratory of Silicon Materials, Cyrus Tang Center for Sensor Materials and Applications,
Department of Materials Science & Engineering, Zhejiang University, Hangzhou, Zhejiang 310027 (P. R.
China).*

Corresponding Authors:

gdqian@zju.edu.cn (G. Qian), yuyang@zju.edu.cn (Y. Yang)

1. Experimental

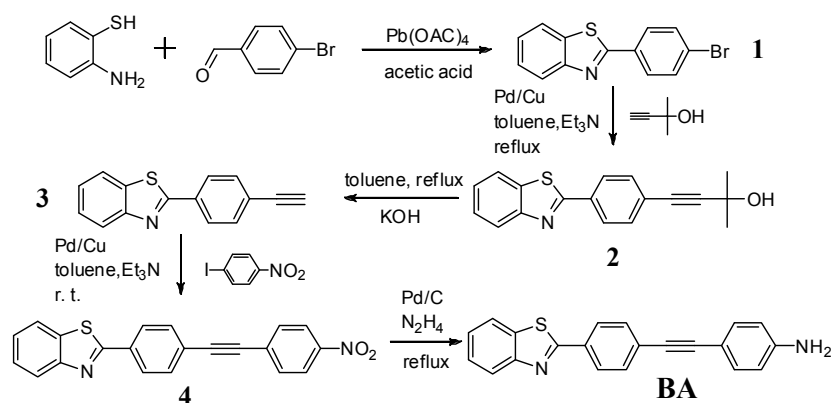
Solvents and reagents were obtained from commercial source and used as received without further purification. ^1H NMR spectra were recorded in CDCl_3 on a 500 MHz Bruker Avance DMX500 spectrometer with tetramethylsilane (TMS) as an internal standard. Elemental analysis was performed using a Thermo Finnigan Flash EA1112 microelemental analyzer. Differential scanning calorimetry (DSC) was performed on a Netzsch Instruments 200 F3 at a heating rate of 10 K/min under nitrogen atmosphere. Fluorescence emission spectra and excitation spectra were obtained on a Hitachi F4600 fluorescence spectrophotometer. UV-vis absorption spectra were obtained using a Perkin-Elmer Lambda spectrophotometer. The Fluorescence decay curves were measured by an Edinburgh Instrument F900.

Fluorescence quantum yield was determined by comparison of the integrated area of the emission spectrum of the sample with that of a known standard, fluorescein ($\Phi = 0.95$ in 0.1 M NaOH). The quantum yield of the sample was calculated according to eq 1

$$\Phi_s = \Phi_r \frac{I_s \text{OD}_r n_s^2}{I_r \text{OD}_s n_r^2} \quad (1)$$

where Φ_s and Φ_r are the fluorescence quantum yield of the sample and the standard; I_s and I_r are the integrated fluorescence intensity of the sample and the standard; OD_s and OD_r are the optical density of the sample and the standard at their respective wavelengths; and n_s and n_r are the refractive index of the sample and the standard, respectively.

Scheme S1 Synthetic Route of BA



2-(4-bromophenyl)benzothiazole (1): 4-bromobenzaldehyde (0.46 g, 2.5 mmol) was stirred into a solution of 2-aminothiophenol (0.31 g, 2.5 mmol) in triethyl phosphate (25 mL). After 10 minutes, acetic acid (2.5 mL) was added into the solution and stirred for a further 10 minutes under temperature 60 °C. Lead (IV) acetate (1.5 g, 3.4 mmol) was added with rapid stirring. After stirred for a further 30 minutes, the solution was cooled to room temperature and extracted with CH₂Cl₂. The organic phase was collected and the solvent was evaporated. The resulting black solid was purified by chromatography using CH₂Cl₂ and petroleum (1:2) as eluent to obtain white solid **1** (0.46 g, 63%). ¹H NMR (500 MHz, CDCl₃): δ 8.07(d, 1H), 7.96(m, 2H), 7.91(d, 1H), 7.63(m, 2H), 7.50(s, 1H), 7.38(m, 2H); ¹³C NMR (500 MHz, CDCl₃): δ 121.85, 123.49, 125.64, 126.70, 129.07, 132.40, 132.65, 135.18, 154.171, 166.86; MS-ESI theoretical: m/z [M+H]⁺=292.0, found: 292.0; Anal. Calcd for C₁₃H₈BrNS: C, 53.81; N, 4.83; H, 2.78. Found: C, 53.81; N, 4.82; H, 2.76; Mp: 132.7 °C.

4-(4-(benzo[d]thiazol-2-yl)phenyl)-2-methylbut-3-yn-2-ol (2): **1** (1.44 g, 5 mmol), Pd(PPh₃)₂Cl₂ (0.14 g, 0.2 mmol), 2-methyl-3-butyn-2-ol (1.26 g, 15 mmol) and CuI (0.038 g, 0.2 mmol) were added into a mixture of Et₃N (2mL) and toluene (8 mL) and refluxed for 12h. The solution was evaporated and purified by chromatography using CH₂Cl₂ and EtOAc (20:1) as eluent, resulting in white crystal **2** (0.64 g, 44%). ¹H NMR (500 MHz, CDCl₃): δ 8.06(d, 1H), 8.03(d, 2H), 7.92(d, 1H), 7.54(t, 3H), 7.40(s, 1H), 2.06(s, 1H), 1.65(s, 6H).

2-(4-ethynylphenyl)benzo[d]thiazole (3): A mixture of **2** (0.59 g, 2 mmol) and KOH (0.56 g, 10 mmol) in toluene (10 mL) was refluxed for 2h. The solution was then extracted with CH₂Cl₂, and the organic phase was combined and evaporated. The resulting black solid was purified by chromatography, using CH₂Cl₂ and petroleum (1:1) as eluent, afforded light yellow solid (0.42 g, 94%). ¹H NMR (500 MHz, CDCl₃): δ 8.06(t, 3H), 7.92(d, 1H), 7.62(d, 2H), 7.52(m, 1H), 7.41(m, 1H), 3.23(s, 1H); ¹³C NMR (500 MHz, CDCl₃): 79.80, 83.26, 121.85, 123.56, 124.85, 125.65, 126.68, 127.54, 132.89, 133.85, 135.30, 154.24, 167.10; MS-ESI theoretical: m/z [M+H]⁺=235.9, found: 236.1; Anal. Calcd for C₁₅H₉NS: C, 76.57; N, 5.95; H, 3.86. Found: C, 76.48; N, 5.87; H, 4.14; Mp: 129.6 °C.

2-(4-((4-nitrophenyl)ethynyl)phenyl)benzo[d]thiazole (4): 1-iodo-4-nitrobenzene (1 g, 4 mmol) and **3** (0.94 g, 4 mmol) were solved into a mixture of Et₃N (4 mL) and toluene (16 mL). CuI (0.038 g, 0.2 mmol) and Pd(PPh₃)₂Cl₂ (0.14 g, 0.2 mmol) were stirred into the solution and heated at 40 °C for 3h under argon atmosphere. The resulting solution was evaporated and purified by chromatography using CH₂Cl₂ and

petroleum (1:1) as eluent to yield yellow solid **4** (1.2 g, 84%). ^1H NMR (500 MHz, CDCl_3): δ 8.29(d, 2H), 8.16(d, 2H), 8.11(d, 1H), 7.96(d, 1H), 7.74(t, 4H), 7.55(t, 1H), 7.45(t, 1H); MS-ESI theoretical: m/z $[\text{M}+\text{H}]^+=357.1$, found: 357.1; Anal. Calcd for $\text{C}_{21}\text{H}_{12}\text{N}_2\text{O}_2\text{S}$: C, 70.77; N, 7.86; H, 3.39. Found: C, 70.38; N, 7.72; H, 3.49; Mp: 248.7 $^\circ\text{C}$.

4-((4-(benzo[d]thiazol-2-yl)phenyl)ethynyl)aniline (BA): 4 (0.72 g, 2 mmol) was dissolved into a 1:1 mixture of EtOH and THF. 5% palladium on carbon (0.27 g) was added into the solution after stirred for 10 minutes under argon atmosphere. The solution was then heated to 60 $^\circ\text{C}$ and hydrazine hydrate (1 mL) was added dropwise during 5 min. The reactants were refluxed for 2 h, filtered and the solvents were evaporated. Recrystallization from EtOH gave light yellow solid (0.62 g, 95%). ^1H NMR (500 MHz, CDCl_3): δ 8.18(d, 1H), 8.09(t, 3H), 7.64(d, 2H), 7.56(t, 1H), 7.49(t, 1H), 7.26(d, 2H), 6.58(d, 2H); ^{13}C NMR (500 MHz, CDCl_3): 86.86, 94.99, 108.03, 114.13, 122.88, 123.40, 126.13, 126.88, 127.24, 127.84, 132.05, 132.09, 133.35, 135.01, 150.44, 154.07, 167.00; MS-ESI theoretical: m/z $[\text{M}+\text{H}]^+=357.1$, found: 357.1; Anal. Calcd for $\text{C}_{21}\text{H}_{14}\text{N}_2\text{S}$: C, 77.27; N, 8.58; H, 4.32. Found: C, 77.38; N, 8.72; H, 4.49; Mp: 265.1 $^\circ\text{C}$.

2. Characterization data

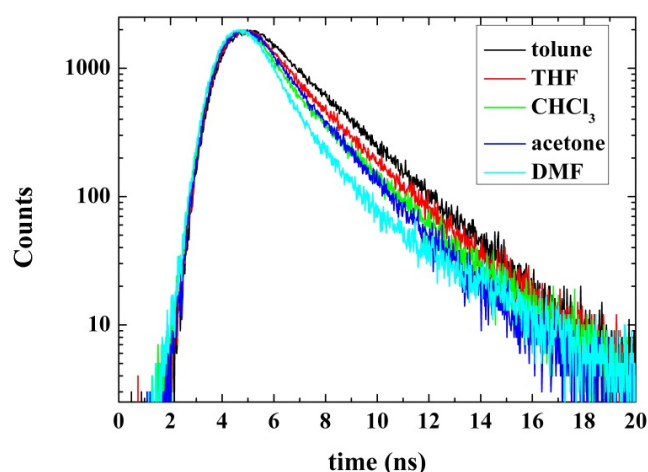


Figure S1 Fluorescence rising and decay curves of BA in toluene, THF, chloroform (CHCl_3), acetone and DMF at the concentration of 10 μM .

Table S1. The main photophysical parameters of BA.^a

solvents	$\epsilon^b/\times 10^4 \text{L}\cdot\text{mol}^{-1}\cdot\text{cm}^{-1}$	τ^c/ns	$\Phi^d/\%$	$\Delta\lambda^e/\text{nm}$
toluene	0.80	2.26	40	79
chloroform	0.74	2.12	38	111
THF	0.85	2.08	18	130
acetone	0.66	2.00	12	142
DMF	0.88	1.84	9	164

a. All the measurements were carried out at the fixed concentration of 10 μM in each solvent, respectively. b. molar extinction coefficient of BA in the corresponding solvent. c. the fluorescence lifetime of BA. d. quantum yield of BA. e. the stokes shift of BA.

Calculation of pKa

The $\text{p}K_a$ of BA was calculated by using the Henderson-Hasselbalch equation:

$$-\log \frac{F_{\max} - F}{F - F_{\min}} = \text{pH} - \text{p}K_a \quad (2)$$

where F_{\max} and F_{\min} are the corresponding maximum and minimum fluorescence intensity, F is the fluorescence intensity observed at a fixed wavelength. The $\text{p}K_a$ of 1.34 indicates BA is suitable for the detection of pH values in strong acid range.

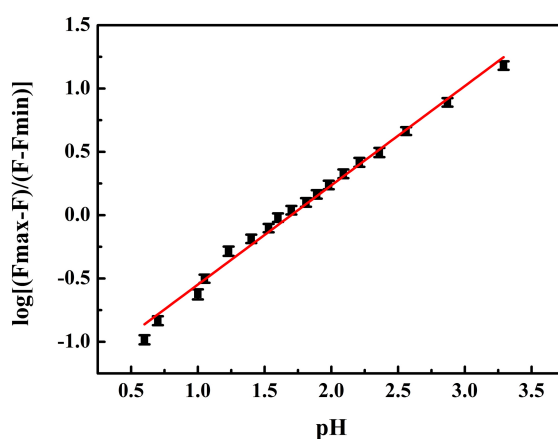


Figure S2 Analysis of fluorescence intensity changes as a function of pH by using Henderson–Hasselbalch equation.

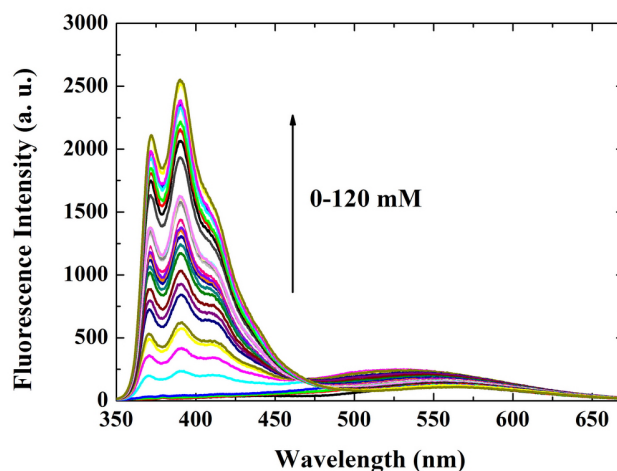


Figure S3 Fluorescence emission spectra of BA in DMF excited at 340 nm, with the addition of various amount (0 ~ 120 mM) of HCl. The concentration of BA was 1 μ M.

Theoretical and computational methods

The molecular geometry of BA and BAH^+ were optimized using density functional theory (DFT) at the B3LYP/6-31G* level.^{S1, S2} The solvent effect on molecular geometries is included by means of the polarizable continuum model (PCM).^{S3, S4} Based on the optimized geometry, the molecular orbitals of BA and BAH^+ were calculated at the same level. All the calculations were performed in Gaussian09 software.^{S5}

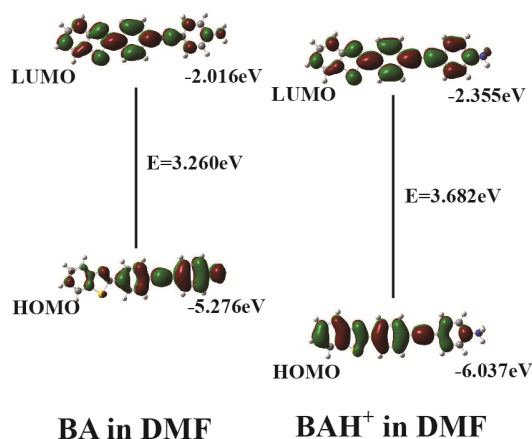


Figure S4 HOMO-LUMO energy levels and the interfacial plots of the molecular orbitals for probe BA and BAH^+ .

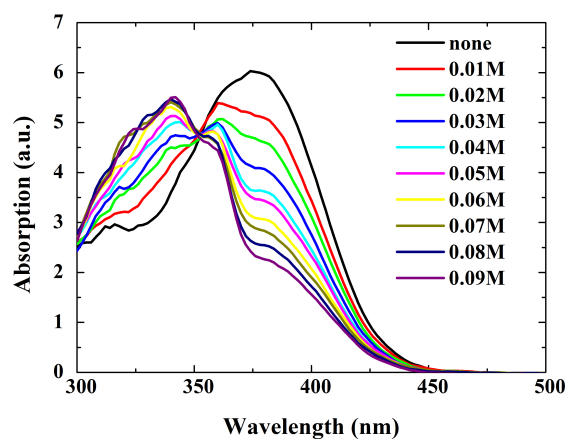


Figure S5 Absorption spectra of BA in DMF at $1 \times 10^{-5} \text{M}$ in the presence of various H^+ concentrations.

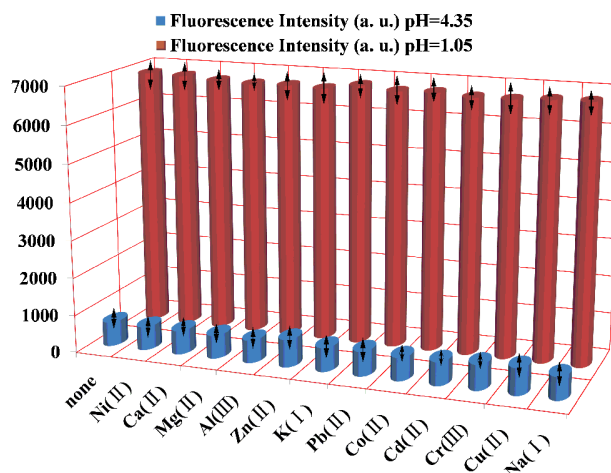


Figure S6 Fluorescence intensities at 390 nm of BA ($1 \mu\text{M}$) in the presence of various metal ions at the pH value of 4.35 and 1.05, respectively (excited at 340 nm). The concentrations of metal ions were all fixed at 1 mM.

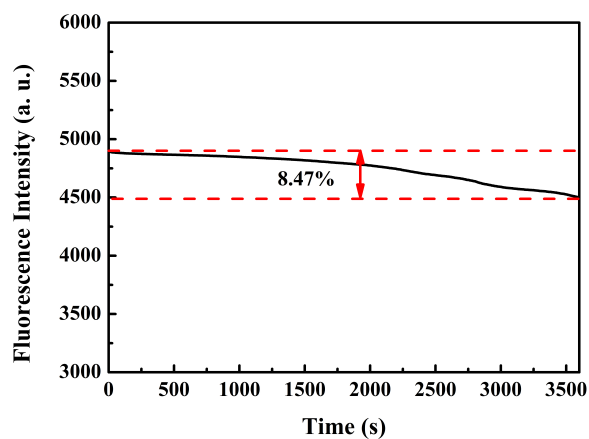


Figure S7. Fluorescence intensity of probe BA at 390 nm with excitation at 340 nm for an hour.

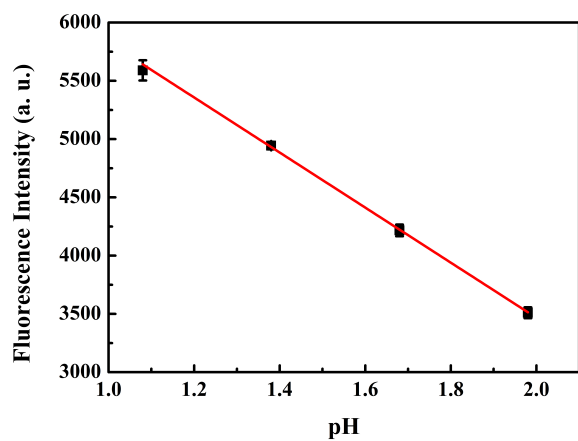


Figure S8. The linear relationship between fluorescence intensity of BA at 390 nm and the pH values in simulated stomach acid. The excitation wavelength is 340 nm.

3. Reference

- S1 W. J. Hehre, R. Ditchfie and J. A. Pople, *J. Chem. Phys.*, 1972, **56**, 2257-2261.
- S2 A. D. Becke, *J. Chem. Phys.*, 1993, **98**, 5648-5652.
- S3 J. Tomasi, B. Mennucci and R. Cammi, *Chem. Rev.*, 2005, **105**, 2999-3094.
- S4 M. Cossi, N. Rega, G. Scalmani and V. Barone, *J. Comput. Chem.*, 2003, **24**, 669-681.
- S5 Gaussian 09, Revision A.01, M. J. Frisch, G. W. Trucks, H. B. Schlegel, G. E. Scuseria, M. A. Robb, J. R. Cheeseman, G. Scalmani, V. Barone, B. Mennucci, G. A. Petersson, H. Nakatsuji, M. Caricato, X. Li, H. P. Hratchian, A. F. Izmaylov, J. Bloino, G. Zheng, J. L. Sonnenberg, M. Hada, M. Ehara, K. Toyota, R. Fukuda, J. Hasegawa, M. Ishida, T. Nakajima, Y. Honda, O. Kitao, H. Nakai, T. Vreven, J. A. Jr. Montgomery, J. E. Peralta, F. Ogliaro, M. Bearpark, J. J. Heyd, E. Brothers, K. N. Kudin, V. N. Staroverov, R. Kobayashi, J. Normand, K. Raghavachari, A. Rendell, J. C. Burant, S. S. Iyengar, J. Tomasi, M. Cossi, N. Rega, J. M. Millam, M. Klene, J. E. Knox, J. B. Cross, V. Bakken, C. Adamo, J. Jaramillo, R. Gomperts, R. E. Stratmann, O. Yazyev, A. J. Austin, R. Cammi, C. Pomelli, J. W. Ochterski, R. L. Martin, K. Morokuma, V. G. Zakrzewski, G. A. Voth, P. Salvador, J. J. Dannenberg, S. Dapprich, A. D. Daniels, O. Farkas, J. B. Foresman, J. V. Ortiz, J. Cioslowski and D. J. Fox, Gaussian, Inc., Wallingford CT, 2009.